Photoinduced Single- versus Double-Bond Torsion in Donor−Acceptor−Substituted *trans*-Stilbenes

Jye-Shane Yang,*,† Kang-Ling Liau,‡ Chung-Yu Hwang,‡ and Chin-Min Wang‡

Department of Chemistry, National Taiwan University, Taipei, Taiwan 10617, and Department of Chemistry, National Central University, Chungli, Taiwan 32054

Received: January 16, 2006; In Final Form: May 11, 2006

The electronic absorption and fluorescence spectra, quantum yields for fluorescence (Φ_f) and trans → cis photoisomerization (Φ_{tc}), and fluorescence lifetimes of *trans*-4-(*N*-arylamino)-4′-cyanostilbenes (**2H**, **2Me**, **2OM**, **2CN**, and **2Xy** with aryl = phenyl, 4-methylphenyl, 4-methoxyphenyl, 4-cyanophenyl, and 2,5-dimethylphenyl, respectively), *trans*-4-(*N*-methyl-*N*-phenylamino)-4′-cyanostilbene (**2MP**), *trans*-4-(*N*,*N*-diphenylamino)-4′-cyanostilbene (**2PP**), *trans*-4-(*N*-methyl-*N*-phenylamino)-4′-nitrostilbene (**3MP**), and three ring-bridged analogues **2OMB**, **2MPB**, and **3MPB** are reported. Whereas fluorescence and torsion of the central double bond account for the excited decay of the majority of these donor−acceptor substituted stilbenes in both nonpolar and polar solvents (i.e., $\Phi_f + 2\Phi_{tc} \sim 1$), exceptions are observed for **2OM**, **3MP**, and **3MPB** in solvents more polar than THF and for **2Me** and **2MP** in acetonitrile as a result of the formation of a weakly fluorescent and isomerization-free twisted intramolecular charge transfer (TICT) state (i.e., $\Phi_f + 2\Phi_{tc} \ll 1$). The TICT state for **2OM**, **2Me**, and **2MP** results from the torsion of the stilbenyl-anilino C−N single bond, but the torsion of the styryl-anilino C−C bond is more likely to be responsible for the TICT state formation of **3MP** and **3MPB**. In conjunction with the behavior of aminostilbenes **1**, a guideline based on the values of Φ_f and Φ_{tc} for judging the importance of a TICT state for *trans*-stilbenes is provided. Accordingly, the TICT state formation is unimportant for the excited decay of *trans*-4-(*N*,*N*-dimethylamino)-4′-cyanostilbene (DCS). In contrast, our results support the previously proposed TICT state for *trans*-4-(*N*,*N*-dimethylamino)-4′-nitrostilbene (DNS).

Introduction

Photoinduced intramolecular charge transfer (ICT) often dictates the excited-state behavior of strong electron donor (D)−acceptor (A) substituted conjugated systems such as 4-(*N*,*N*-dimethylamino)benzonitrile (DMABN) and *trans*-4-(*N*,*N*-dimethylamino)-4′-cyanostilbene (DCS). A controversial but fundamentally important issue associated with the ICT process is the geometry and dynamic properties of the low-lying ICT states.[1−10] In nonpolar solvents, it is conceivable that the ICT state is dominated by D−A mesomeric interactions and thus favors a planar geometry (PICT).[4−7] However, in polar solvents, the opposite extreme of PICT, referred to as TICT, where the D and A fragments are twisted and nearly electronically decoupled, might become energetically more favorable (Figure 1).[2,3,8] It is assumed that a TICT state allows a larger charge separation and thus possesses a larger molecular dipole moment and in turn gains a greater solvation in polar solvents. The currently proposed TICT state for DMABN results from the twisting of the dimethylamino (D)−benzonitrilo (A) C−N bond,[2,3] and for DCS, it is from the twisting of the anilino (D)−styryl (A) C−C bond.[8] In principle, the radiative transition between the TICT and the ground states (S_0) is forbidden,[2] corresponding to a precursor−successor relationship for TICT state formation and a lower fluorescence quantum yield (Φ_f) for its decay. Whereas DMABN shows dual fluorescence with the ICT fluorescence satisfactorily conforming to such a TICT scenario,[2] discrepancies are found in the case of DCS, which is highly emissive and lacks a distinct steady-state dual fluorescence.[5−8] Although the latter has been attributed to either a large vibronic mixing of the TICT state with the other allowed states or an incomplete twisting of the single bond (i.e., twisted angle <90°),[8] firm conclusions on the structure and dynamics of the ICT state for DCS remain to be established.

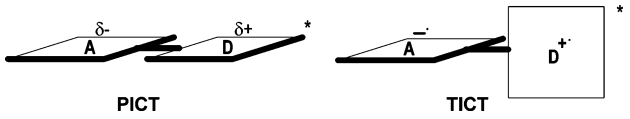

Figure 1. Schematic drawing of geometries for PICT and TICT states for donor (D)−acceptor (A) substituted conjugated systems.

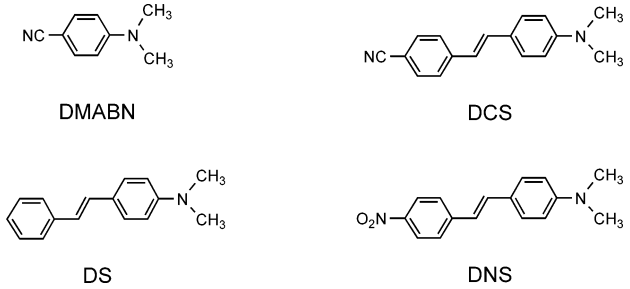

Unlike the controversial issue of multiple excited singlet states due to torsion of a specific single bond, singlet state olefinic bond torsion that leads to formation of a short-lived twisted intermediate (i.e., $^1t^* \rightarrow {}^1p^*$) is a well-known photochemical process for *trans*-stilbenes.[11−15] Assuming that trans and cis

* Corresponding author. E-mail: jsyang@ntu.edu.tw.
† National Taiwan University.
‡ National Central University.

10.1021/jp060296g CCC: $33.50
Published on Web 06/14/2006

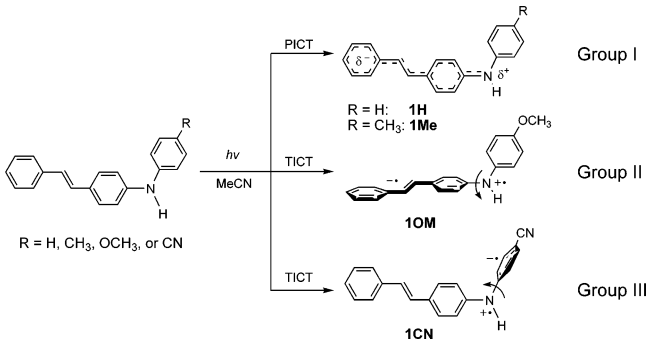

Figure 2. Substituent (R)-dependent structures of ICT states for *N*-aryl substituted *trans*-4-aminostilbenes (**1**) in acetonitrile.

isomers are populated 50% each from ^{1}p*, the quantum yield for double-bond torsion (Φ_d) can be obtained from that for trans → cis photoisomerization (Φ_{tc}): namely, $\Phi_d = 2\Phi_{tc}$. Although photoisomerization can occur via the triplet state as well as the singlet state, the triplet-state mechanism has been shown to be unimportant for DCS due to inefficient $S_1 \rightarrow T_1$ intersystem crossing.[7] Since fluorescence and singlet-state isomerization account for the excited decay of DCS in both nonpolar and polar solvents (i.e., $\Phi_f + 2\Phi_{tc} \sim 1.0$),[6,7] as observed for many other substituted *trans*-stilbenes,[11−15] the necessity of invoking a TICT state for DCS is again questioned. In particular, the excited-state hypersurface for the proposed TICT → ^{1}p* process is poorly defined and not well understood.[8]

We recently reported that the *N*-aryl amino conjugation effect can be a useful probe for differentiating a TICT from a PICT state for *trans*-4-aminostilbenes (e.g., **1H**, **1Me**, **1OM**, and **1CN**).[16] Our approach relies on the fact that the fluorescence properties of *N*-aryl substituted *trans*-4-aminostilbenes are sensitive to the degree of conjugation between the D and the A groups in the excited states.[17] In conjunction with the properties of the ring-bridged model compounds, we have shown that TICT state formation is possible when the amino donor is sufficiently strong, such as the *N*-(4-methoxylphenyl)amino group in **1OM** (Figure 2). However, the TICT state for **1OM** results from the twisting of the stilbenyl (A)−anilino (D) C−N bond rather than from the styryl-anilino C−C bond as previously proposed for *trans*-4-(*N*,*N*-dimethylamino)stilbene (DS)[18] and DCS.[8] In addition, compound **1CN** was shown to have a DMABN-like TICT state, where the aminostilbene group functions as the electron donor (Figure 2). Independent of the bond involved in the TICT state, TICT state formation in both cases results in a low quantum yield for both fluorescence and iosmerization (i.e., $\Phi_f + 2\Phi_{tc} \ll 1.0$), indicating that its decay is mainly due to internal conversion.[19] Inspection of the solvent-dependent fluorescence behavior of DS also revealed that it resembles that of the TICT-free species **1Me** and **1H** rather than that of **1OM** or **1CN**. This in turn indicates that the *N*,*N*-dimethylamino group alone does not promote formation of a stable TICT state for *trans*-stilbene.

In view of the informative *N*-aryl amino conjugation effect on the excited-state conformation of D-only substituted stilbenes,[16] we extended its application to D−A substituted stilbenes, particularly to DCS-related systems. In this context, we have investigated a series of *N*-aryl substituted *trans*-4-amino-4′-cyanostilbenes (**2**). Regarding the different excited-state behavior of *trans*-4-(*N*,*N*-dimethylamino)-4′- nitrostilbene (DNS)[9,10] versus DCS, the nitro species **3MP** was also investigated and compared with **2MP**. For further information, three ring-bridged derivatives (**2OMB**, **2MPB**, and **3MPB**) were also studied. We report herein that the TICT state for **2** possesses the same characteristics of low Φ_f and Φ_{tc} as that for **1**, and thus, the parameters of $\Phi_f + 2\Phi_{tc}$ could also be a TICT probe for D−A substituted *trans*-stilbenes. According to the nature of their ICT states in acetonitrile, these compounds are divided into four different groups (Groups I−IV), which possess a PICT, a stilbenyl-anilino C−N bond TICT, a DMABN-like TICT, and a styryl-anilino C−C bond TICT state, respectively. Application of the same criteria suggests that the fluorescent ICT state for DCS in acetonitrile is planar rather than twisted, but the presence of a stronger electron-withdrawing NO_2 group in DNS favors TICT state formation.

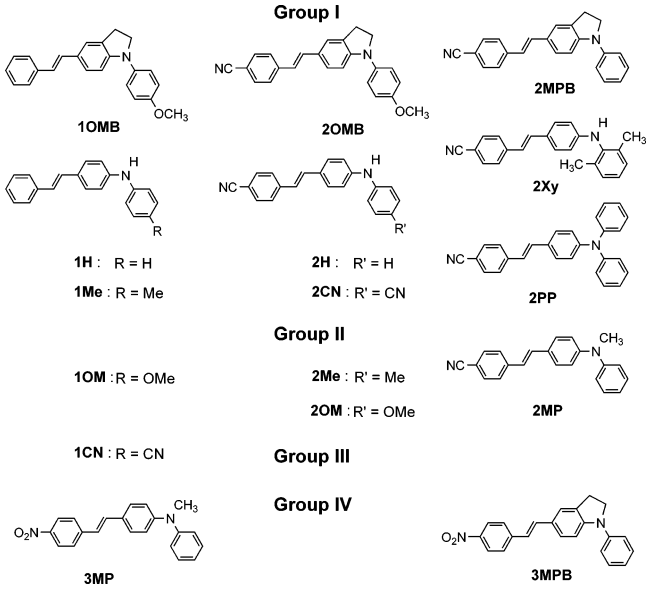

Experimental Procedures

Materials. Amino-cyano disubstituted stilbenes **2** were prepared by palladium-catalyzed amination reactions between *trans*-4-bromo-4′-cyanostilbene and the corresponding commercially available arylamines.[20] The amino-nitro disubstituted stilbene **3MP** was also obtained by this method by replacing the disubstituted stilbene with *trans*-4-bromo-4′-nitrosilbene. Typical procedures have been previously reported for the synthesis of aminostilbenes **1**.[17] The synthesis of ring-bridged compounds **2OMB**, **2MPB**, and **3MPB** also followed the same strategy previously reported for compound **1OMB**.[16] All the new compounds were identified by ^{1}H NMR, ^{13}C NMR, MS, IR, and/or elemental analysis. These data are provided as Supporting Information. Solvents for spectra and quantum yield measurements all were HPLC grade and used as received.

Methods. Electronic spectra were recorded at room temperature (23 ± 1 °C). UV spectra were measured on a Jasco V-530 double beam spectrophotometer. Fluorescence spectra were recorded on a PTI QuantaMaster C-60 spectrofluorometer and corrected for the response of the detector. The optical density of all solutions was about 0.1 at the wavelength of excitation. The fluorescence spectra at other temperatures were measured in an Oxford OptistatDN cryostat with an ITC502 temperature controller. A N_2-bubbled solution of anthracene ($\Phi_f = 0.27$ in hexane)[21] was used as a standard for the fluorescence quantum yield determinations of aminostilbenes under N_2-bubbled conditions with solvent refractive index correction. An error of ±10% is estimated for the fluorescence quantum yields. Fluorescence decays were measured at room temperature by means of a PTI Timemaster apparatus with a gated hydrogen arc lamp using a scatter solution to profile the instrument response function. The

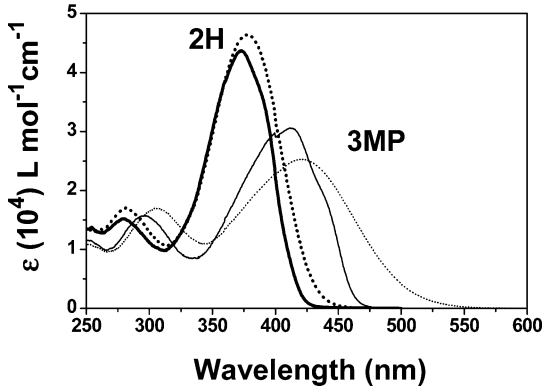

Figure 3. Electronic absorption spectra of **2H** (thicker lines) and **3MP** in hexane (solid curves) and acetonitrile (dotted curves).

goodness of nonlinear least-squares fit was judged by the reduced χ^2 value (<1.2 in all cases), the randomness of the residuals, and the autocorrelation function. Quantum yields of trans → cis photoisomerization were measured on optically dense outgassed solutions at 350 nm using a 75 W Xe arc lamp and monochromator. Compound **1H** was used as a reference standard ($\Phi_{tc} = 0.34$ in dichloromethane).[16] The concentration of the solute is ca. 10^{-3} M for all cases. The effect of concentration on the photoisomerization was studied with **2OM** in dichloromethane and **2Me** in acetonitrile using another solution of lower concentrations ($\sim 4 \times 10^{-5}$ M). Observation of the same results rules out the possibility of interference from bimolecular events. The extent of photoisomerization (<10%) was determined using HPLC analysis (Waters 600 Controller and 996 photodiode array detector, Thermo APS-2 Hypersil, heptane and ethyl acetate mixed solvent). The reproducibility error was <10% of the average. MOPAC-AM1 calculations were performed on a personal computer using the algorithms supplied by the package of Quantum CAChe Release 3.2, a product of Fujitsu Limited.

Results

Electronic Spectra. All the aminostilbenes **1**−**3** in hexane and acetonitrile display a single intense long-wavelength absorption band. The spectra for aminostilbenes **1** have been reported,[16,17] and typical spectra represented by the cases of **2H** and **3MP** are shown in Figure 3. The corresponding fluorescence spectra are more or less structured in hexane but structureless in acetonitrile. Figure 4 shows the fluorescence spectra of **2H**, **2Me**, **2OM**, and **2CN** in a variety of solvents. Spectral data in hexane and acetonitrile for the absorption maxima (λ_{abs}), fluorescence maxima (λ_f), the half-bandwidth ($\Delta\nu_{1/2}$), the 0,0 transitions ($\lambda_{0,0}$), and the Stokes shift ($\Delta\nu_{st}$) are reported in Table 1. For comparison, the data for DCS,[6] DNS,[9] **1H**, **1OM**, and **1OMB**[16] are included.

When compared with aminostilbenes **1**, amino-cyano disubstituted stilbenes **2** with the same amino donors are red-shifted in both the absorption and the fluorescence spectra, and the Stokes shift is similar in hexane but larger in acetonitrile. Such spectral differences reflect the elongated length of π-conjugation and the stronger ICT character for **2** versus **1** (vide infra). Nonetheless, the spectra of **1** and **2** have several features in common: (a) the absorption spectra are essentially structureless in both hexane and acetonitrile, but the fluorescence spectra show vibrational structure in hexane. Since a more structured spectrum indicates better correspondence between excited-state and ground-state geometries, the structure in hexane is more planar in the excited state than in the ground state. (b) The

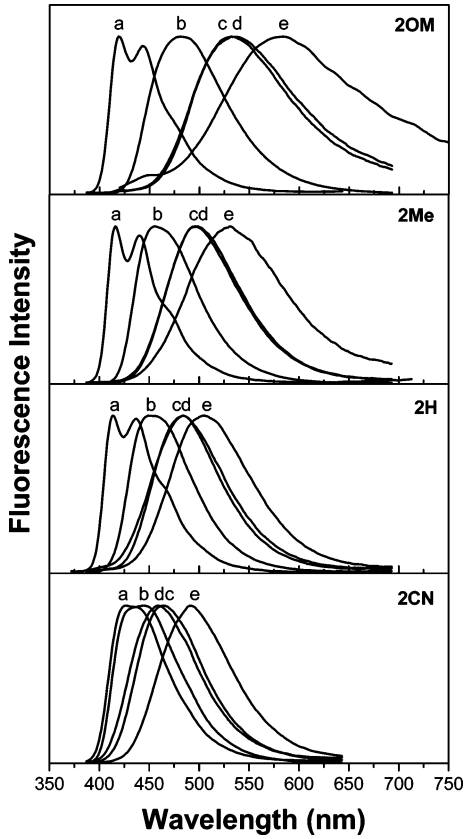

Figure 4. Normalized fluorescence spectra of **2H**, **2Me**, **2OM**, and **2CN** in (a) hexane, (b) toluene, (c) THF, (d) dichloromethane, and (e) acetonitrile.

solvatochromic shift on going from hexane to acetonitrile is rather small for the absorption spectra but is large for the fluorescence spectra. The former suggests a small difference in dipole moments between the Franck−Condon excited state and the ground state, and the latter indicates a high polarity for the fluorescing state as a result of pronounced ICT. (c) The shifts of λ_{abs} as a result of changes in the amino substituents are parallel in terms of the magnitude and direction. Specifically, electron-donating and electron-withdrawing substituents at the para position of the *N*-phenyl group shift the λ_{abs} toward the red (e.g., **2OM** and **2Me** vs **2H**) and to the blue (e.g., **2CN** vs **2H**), respectively. In other words, the stronger the amino electron donor, the longer the wavelength of the absorption maximum is. This is consistent with our previous ZINDO[22] calculations on **2H**,[17] which revealed that the long-wavelength absorption band is essentially due to a one-electron transition from the HOMO (amino nitrogen) to the LUMO (stilbene).

The dipole moment (μ_e) of the fluorescent state can be estimated from the slope (m_f) of the plot of the energies of the fluorescence maxima against the solvent parameter Δf according to eq 1[23]

$$\nu_f = -[(1/4\pi\epsilon_0)(2/hca^3)][\mu_e(\mu_e - \mu_g)]]\Delta f + \text{constant} \quad (1)$$

where

$$\Delta f = (\epsilon - 1)/(2\epsilon + 1) - 0.5(n^2 - 1)/(2n^2 + 1) \quad (2)$$

and

$$a = (3M/4N\pi d)^{1/3} \quad (3)$$

TABLE 1: Maxima of UV Absorption (λ_{Abs}) and Fluorescence (λ_f), Fluorescence-Band Half-Width ($\Delta\nu_{1/2}$), 0,0 Transition ($\lambda_{0,0}$), and Stokes Shifts ($\Delta\nu_{st}$) of Aminostilbenes 1−3 in Hexane (Hex) and Acetonitrile (MeCN)[a] and Those of DCS and DNS in Cyclohexane (CH) and MeCN

compd	solvent	λ_{abs} (nm)	λ_f (nm)[b]	$\Delta\nu_{1/2}$ (cm^{-1})	$\lambda_{0,0}$ (nm)[c]	$\Delta\nu_{st}$ (cm^{-1})[d]
1H[e]	Hex	346	381 (399)	2956	370	2655
	MeCN	351	442	3547	393	5785
1OM[e]	Hex	349	389 (409)	2782	378	2946
	MeCN	356	502	6218	398	8170
1OMB[e]	Hex	367	408 (430)	2362	398	2738
	MeCN	373	483	3429	423	6106
2H	Hex	373	414 (437)	3513	401	2655
	MeCN	379	504	3670	432	6544
2Me	Hex	376	416 (440)	3064	405	2557
	MeCN	382	531	3999	440	7346
2OM	Hex	376	419 (443)	3205	407	2729
	MeCN	384	583	4935	449	8889
2OMB	Hex	400	447 (475)	2415	436	2629
	MeCN	408	590	3670	484	7561
2CN	Hex	371	427 (439)	3452	405	3535
	MeCN	371	491	3485	426	6588
2MP	Hex	381	422 (447)	2801	411	2550
	MeCN	384	527	3905	441	7066
2MPB	Hex	397	435 (462)	2443	426	2200
	MeCN	399	552	3088	467	6947
2PP	Hex	390	430 (457)	2561	420	2385
	MeCN	388	542	3906	448	7323
2Xy	Hex	367	(418) 436	3478	401	4312
	MeCN	375	509	3258	437	7020
3MP	Hex	413	494	3638	452	3970
	MeCN	422	>800			
3MPB	Hex	428	(485) 512	3340	469	3833
	MeCN	439	>800			
DCS[f]	CH	380	418			
	MeCN	383	530			
DNS[g]	CH	417	(470) 502			
	MeCN	435	>850			

[a] Fluorescence data are from corrected spectra. [b] Maxima of the second vibronic bands are given in parentheses. [c] The value of $\lambda_{0,0}$ was obtained from the intersection of normalized absorption and fluorescence spectra. [d] $\Delta\nu_{st} = \nu_{abs} - \nu_f$. [e] Data from ref 16. [f] Data from ref 6. [g] Data from ref 9.

TABLE 2: Ground- and Excited-State Dipole Moments for 2

compd	a (Å)[a]	m_f (cm^{-1})[b]	μ_g (D)[c]	μ_e (D)
2CN	5.03	9882	4.19	13.5 ± 0.9
2Xy	5.05	9733	6.20	14.7 ± 1.0
2H	4.90	12560	4.84	14.8 ± 0.6
2MP	4.97	12817	4.91	15.2 ± 0.5
2MPB	5.04	13393	4.95	15.8 ± 0.6
2Me	4.97	14565	5.11	16.1 ± 0.5
2OM	5.06	15832	3.93	16.4 ± 0.8
2PP	5.12	13454	5.85	16.6 ± 0.6
2OMB	5.19	14620	4.62	16.7 ± 0.7

[a] Onsager radius calculated by eq 3 with $d = 1.0$ g/cm^3 for all compounds except for **2PP** ($d = 1.1$ g/cm^3). [b] Calculated based on eq 1. [c] Calculated by use of AM1.

where ν_f is the fluorescence maximum; μ_g is the ground-state dipole moment; a is the solvent cavity (Onsager) radius, which was derived from the Avogadro number (N), molecular weight (M), and density (d); and ϵ, ϵ_0, and n are the solvent dielectric constant, the vacuum permittivity, and the solvent refractive index, respectively. The value of μ_g was calculated using the MOPAC-AM1 algorithm.[24] The calculated dipole moments for **2** are summarized in Table 2, and they are arranged in an order of increasing μ_e value, namely, **2CN** < **2Xy** < **2H** < **2MP** < **2MPB** < **2Me** < **2OM** < **2PP** < **2OMB**. The relative order among **2CN**, **2H**, **2Me**, and **2OM** is consistent with the relative electron-donating ability of the *N*-arylamino group based on the Hammett substituent constants.[25] A smaller value of μ_e for **2Xy** versus **2H** resembles the case of **1Xy** versus **1H** as a result of a less planar structure due to the bulkier *N*-aryl group.[17] The solvatofluorochromic shift is similar for the pair of **2MP** and **2MPB** and for that of **2OM** and **2OMB**, indicating that a restriction of the stilbenyl-anilino C−N bond rotation imposes only a small effect on the polarity of the fluorescent ICT state.

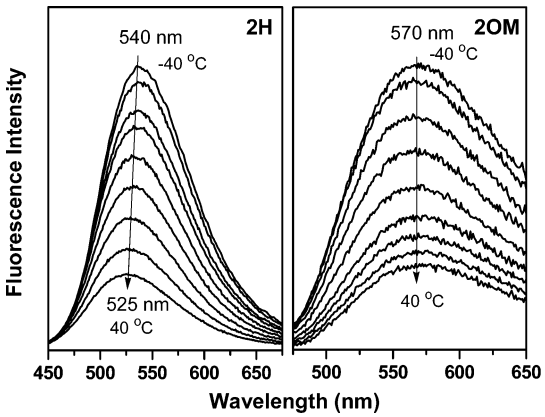

Figure 5. Temperature dependence of the fluorescence spectra of **2H** and **2OM** in acetonitrile/THF (9:1) recorded at intervals of 10 °C between −40 and 40 °C.

The dependence of the fluorescence spectra of **2H** and **2OM** in methylcyclohexane and mixed acetonitrile/THF (9:1) on temperature was investigated. Addition of 10% THF to the acetonitrile solutions prevents substrate aggregation or precipitation at low temperature. The fluorescence intensity for all four cases decreases monotonically upon heating from −40 to 40 °C.[26] Figure 5 shows the spectra of **2H** and **2OM** in acetonitrile/THF (9:1), where a small blue-shift of λ_f accompanies the decrease in intensity for **2H** but not for **2OM**. For comparison, a decrease of fluorescence intensity and a slight blue-shift in λ_f are also observed for **1H** in both hexane and acetonitrile and for **1OM** in hexane. However, for **1OM** in acetonitrile, the fluorescence intensity increases as the temperature is increased.[17]

Quantum Yields and Lifetimes. Fluorescence quantum yields for **2** and **3** were determined in hexane, dichloromethane, and acetonitrile (Table 3). In some cases, data in THF are also reported. Values of Φ_f for DCS and DNS in cyclohexane, methyltetrahydrofuran (MTHF), and acetonitrile are included in Table 3. While the majority of these D−A substituted stilbenes possess a larger value of Φ_f in more polar solvents, an opposite trend with a particularly low value in acetonitrile is observed for **2OM**, **3MP**, and **3MPB**. In contrast, the Φ_f value of **2Me** and **2MP** increases first on going from hexane to dichloromethane but then decreases on going from dichloromethane to acetonitrile, and the resulting value in the latter is smaller than that in hexane.

Quantum yields for trans → cis photoisomerization for **2** and **3** along with DCS and DNS in selected solvents are reported in Table 3. Except for **2OM**, **3MP**, and **3MPB** in THF and more polar solvents[27] and for **2Me** and **2MP** in acetonitrile that show the behavior of $\Phi_f + 2\Phi_{tc} \ll 1.0$, the sum of $\Phi_f + 2\Phi_{tc}$ is within the experimental error of 1.0 (±0.2) for all cases. Apparently, decay channels other than fluorescence and photoisomerization should be taken into account for the former cases. It should be noted that DCS also possesses a behavior of $\Phi_f + 2\Phi_{tc} \sim 1.0$ in both cyclohexane and acetonitrile, and so is DNS in cyclohexane; however, the sum of $\Phi_f + 2\Phi_{tc}$ is only 0.16 for DNS in MTHF.

TABLE 3: Quantum Yields for Fluorescence (Φ_f) and Photoisomerization (Φ_{tc}), Fluorescence Decay Times (τ_f), Rate Constants for Fluorescence Decay (k_f), and Nonradiative Decay (k_{nr}) for 2, 3, DCS, and DNS in Solution

compd	solvent	Φ_f	Φ_{tc}	τ_f (ns)[a]	k_f (10^8 s^{-1})	k_{nr} (10^8 s^{-1})
2H	Hex	0.11	0.45[b]	0.22	5.0	40.5
	CH_2Cl_2	0.23	0.44	0.37	6.2	20.8
	MeCN	0.35	0.33[c]	0.87	4.0	7.5
2Me	Hex	0.18		0.21	8.6	39.0
	CH_2Cl_2	0.35	0.34	0.81	4.3	8.0
	MeCN	0.13	0.02[d]	0.44	3.0	19.8
2OM	Hex	0.25	0.27[b]	0.43	5.8	17.4
	THF	0.05	<0.01	0.43	1.2	22.1
	CH_2Cl_2	0.06	<0.01	0.22	2.7	42.7
	MeCN	<0.005	<0.01			
2OMB	Hex	0.37		0.86	4.3	7.3
	THF	0.64	0.17	2.03	3.2	1.8
	CH_2Cl_2	0.65	0.16	2.23	2.9	1.6
	MeCN	0.62	0.18	2.54	2.4	1.5
2CN	Hex	0.29[d]		0.39	7.4	18.2
	CH_2Cl_2	0.22	0.34[e]	0.42	5.2	18.6
	MeCN	0.27	0.30[f]	0.44	6.1	16.6
2MP	Hex	0.19	0.42[b]	0.28	6.8	28.9
	CH_2Cl_2	0.36	0.37	0.72	5.0	8.9
	MeCN	0.16	0.12	0.76	2.1	11.1
2MPB	Hex	0.29		0.55	5.3	12.9
	CH_2Cl_2	0.46	0.29	1.22	3.8	4.4
	MeCN	0.65	0.18	1.90	3.4	1.8
2PP	Hex	0.79		1.48	5.3	1.4
	CH_2Cl_2	0.93		2.54	3.7	0.3
	MeCN	0.92	0.05	3.43	2.7	0.2
2Xy	Hex	0.03		<0.1	>3.0	>97.0
	CH_2Cl_2	0.05	0.51	0.16	3.1	59.4
	MeCN	0.09	0.49[e]	0.20	4.5	45.5
3MP	Hex	0.33		0.65	5.1	10.3
	THF	0.30	0.01	1.79	1.7	3.9
	CH_2Cl_2	<0.005				
	MeCN	<0.005				
3MPB	Hex	0.56		1.68	3.3	2.6
	THF	0.26	0.02	3.33	0.8	2.2
	CH_2Cl_2	0.06				
	MeCN	<0.005				
DCS[g]	cHex	0.03	0.45	0.085	3.53	114
	MTHF	0.06	0.4			
	MeCN	0.13	0.4	0.52	2.5	16.7
DNS[h]	cHex	0.33	0.28			
	MTHF	0.15	0.004			
	MeCN	<0.002				

[a] The value of τ_f was determined with excitation and emission around the spectral maxima, unless otherwise noted. [b] Containing 20% of THF by reason of solubility. [c] Containing 6% of THF by reason of solubility. [d] Containing 10% of THF by reason of solubility. [e] Containing 8% of THF by reason of solubility. [f] Containing 12% of THF by reason of solubility. [g] Data from ref 6. [h] Data from ref 9.

The room temperature fluorescence lifetimes (τ_f) and rate constants for fluorescence ($k_f = \Phi_f\tau_f^{-1}$) and the overall nonradiative deactivation processes ($k_{nr} = (1 - \Phi_f)\tau_f^{-1}$) for **2** and **3** in selected solvents are provided in Table 3. All decays can be well-fit by single-exponential functions, although more than one planar conformer is expected for all cases, except for **2PP**. For substrates with $\Phi_f + 2\Phi_{tc} \sim 1.0$, their k_f and k_{nr} are both smaller in acetonitrile than in hexane. For comparison, aminostilbenes **1** also display smaller values of k_f in acetonitrile versus hexane, but the opposite was observed for k_{nr}.

To gain further insight into solvent effects on the photoisomerization of D−A versus D-only substituted stilbenes, the temperature-dependent fluorescence lifetimes of **1H** and **2H** in methylcyclohexane and in mixed acetonitrile/THF (9:1) were determined. Assuming that C═C torsion was the only activated singlet-decay process and that k_f was temperature independent,

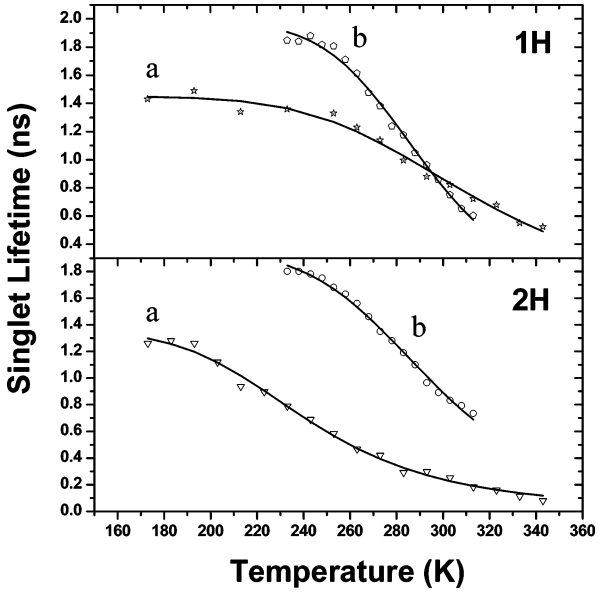

Figure 6. Temperature-dependent fluorescence lifetimes for **1H** and **2H** in (a) methylcyclohexane and (b) acetonitrile/THF (9:1) and nonlinear fits to eq 4.

TABLE 4: Activation Parameters for 1H and 2H in Methylcyclohexane and Acetonitrile/THF (9:1)

compd	solvent	$10^{-8}\,\Sigma k$ [a,b] (s^{-1})	log A[c]	E_a[c] (kcal/mol)	$10^{-8}k_d$ (s^{-1})[d,e]
1H	MCH	6.9 ± 0.3 (5.7)	12.3 ± 0.1	4.9 ± 0.5	4.9 (5.5)
	MeCN/THF	5.1 ± 0.1 (3.5)	14.4 ± 0.1	7.6 ± 0.6	6.2 (6.9)
2H	MCH	7.4 ± 0.1 (5.0)	12.4 ± 0.1	3.9 ± 0.3	30.6 (40.5)
	MeCN/THF	5.1 ± 0.1 (4.0)	13.3 ± 0.1	6.3 ± 0.4	5.0 (7.5)

[a] Sum of the nonactivated singlet decay processes. [b] The value given in parentheses is k_f derived from Φ_f and τ_f measured at room temperature.[30] [c] Activation parameters for singlet activated decay from nonlinear fitting of temperature-dependent lifetimes (Figure 6). [d] Room temperature double-bond torsional rate calculated from A and E_a. [e] The value given in parentheses is k_{nr} derived from $(1 - \Phi_f)$ and τ_f measured at room temperature.[30]

the torsional barrier can be obtained from nonlinear fitting of the fluorescence lifetimes using eq 4[28,29]

$$\tau_f(T) = 1/[\Sigma k + A\exp(-E_a/RT)] \quad (4)$$

where Σk is the sum of all nonactivated processes (fluorescence and intersystem crossing), and A and E_a are the preexponential and activation energy for the activated process, respectively. These results are shown in Figure 6, and the activation parameters are reported in Table 4. The value of E_a is larger for both **1H** and **2H** in polar (i.e., MeCN/THF) than in nonpolar (i.e., MCH) solvents, although the value of Φ_{tc} is larger for **1H** in more polar solvents[16] but it is larger for **2H** in less polar solvents. When compared with the k_f and k_{nr} values derived from the fluorescence quantum yields and lifetimes (Table 3), the room temperature values of Σk and k_d are similar to those of k_f and k_{nr}, respectively, for all four cases.[30] This suggests that the nonactivated and activated singlet decay processes for **1H** and **2H** in both nonpolar and polar solvents are mainly fluorescence and photoisomerization, respectively. The somewhat larger values of Σk versus k_f along with the somewhat smaller values of k_d versus k_{nr} for all cases indicate the presence of a minor nonactivated decay process, which can be attributed to the $S_1 \rightarrow T_1$ intersystem crossing, followed by trans → cis photoisomerization. We recently showed that photoisomerization via the triplet state is nonnegligible for *N*-aryl substituted 4-aminostilbenes.[31]

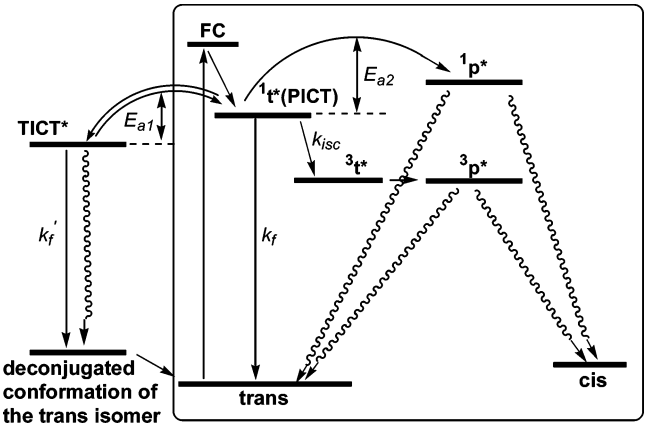

Figure 7. Simplified scheme for the formation and decay of the fluorescent ICT state of aminostilbenes **1**−**3**, where the portion in the square corresponds to the conventional two-state (^{1}t* (PICT) and ^{1}p*) model.

Discussion

Our previous studies on *N*-aryl substituted aminostilbenes **1** have suggested that TICT state formation depends on the electronic properties of the *N*-aryl group (Figure 2).[16] The arguments in favor of the participation of a TICT state for **1OM** (Group II) and **1CN** (Group III) but not for **1H** and **1Me** (Group I) in polar solvents such as acetonitrile are summarized as follows: (1) fluorescence and torsion of the central double bond accounts for the excited singlet decay for all four compounds in hexane and for **1H** and **1Me** in acetonitrile (i.e., $\Phi_f + 2\Phi_{tc} \sim 1.0$), but other nonradiative decay pathways are dominant for **1OM** and **1CN** in acetonitrile because $\Phi_f + 2\Phi_{tc} \ll 1.0$. (2) In acetonitrile, **1H** and **1Me** display a single fluorescence emission band with a half-bandwidth less than 3900 cm^{-1}, whereas the fluorescence bands are unusually broad in the cases of **1OM** ($\Delta\nu_{1/2} \sim 6200$ cm^{-1}) and **1CN** ($\Delta\nu_{1/2} \sim 8100$ cm^{-1}). In fact, **1CN** shows dual fluorescence in polar solvents, indicating the presence of more than one emitting singlet state. (3) The value of Φ_f drops by a factor of ~100 for **1OM** and **1CN** on going from hexane to acetonitrile, but the corresponding change in Φ_f for **1H** and **1Me** is less than 2-fold. Apparently, the new emitting state (i.e., the TICT state) is of weak fluorescence and inefficient photoisomerization. (4) The fluorescence intensity for **1OM** and **1CN** in acetonitrile increases with increasing temperature, which corresponds to an equilibrium between the TICT and the ^{1}t* state. In contrast, their fluorescence intensity in hexane is either decreased or unchanged upon raising the temperature, corresponding to an activated and inactivated photoisomerization process, respectively. (5) As indicated by the ring-bridged model compound **1OMB**, the previous discrepancies in fluorescence properties between **1H** (or **1Me**) and **1OM** disappear when the twisting of the stilbenyl-anilino C−N bond in **1OM** is restricted. A similar phenomenon was observed for **1CN** when the rotation of the aniline-benznitrilo C−N was inhibited, indicating the formation of a DMABN-like TICT state. All this information suggests that a two-state model (^{1}t* (PICT) and ^{1}p*) is sufficient to account for the photochemical behavior of **1H** and **1Me**, but a three-state model (^{1}t*, ^{1}p*, and TICT) is required for **1OM** and **1CN** (Figure 7). It should be noted that the structure of the TICT state for **1OM** is very different from that for **1CN** in terms of the bond that twists and the direction of ICT, but their formation and decay mechanisms are essentially the same. Therefore, a PICT state of *trans*-aminostilbenes would conform to $\Phi_f + 2\Phi_{tc} \sim 1.0$, and the presence of a TICT state would lead to $\Phi_f + 2\Phi_{tc} \ll 1.0$, presumably due to efficient internal conversion from S_1 to S_0.[19]

In principle, the additional CN group in **2OM** versus **1OM** should further facilitate TICT state formation. Provided that the decay mechanism of the TICT state for **2OM** is similar to that for **1OM**, a result of $\Phi_f + 2\Phi_{tc} \ll 1$ was expected. Indeed, **2OM** has extremely low values of Φ_f and Φ_{tc} in acetonitrile (Table 3). When the rotation of the stilbenyl-anilino C−N bond is restricted, as shown by **2OMB**, the behavior of $\Phi_f + 2\Phi_{tc} \sim 1.0$ is observed. We can thus conclude that there exists a TICT state for **2OM** in THF and more polar solvents and, as is the case of **1OM** (Figure 2),[16] it results from the twisting of the stilbenyl-anilino C−N bond (i.e., Group II). However, there are two apparent differences in the fluorescence spectra of **2OM** versus **1OM**: (1) the half-bandwidth (4935 cm^{-1}) for **2OM** in acetonitrile is much smaller than that for **1OM** (6218 cm^{-1}) (Table 1). This appears to suggest that the TICT state of D−A substituted *trans*-stilbenes is much less fluorescent than that of the D-only analogues. In other words, the observed fluorescence for **2OM** is predominately from the ^{1}t* (PICT) state in all solvents, but for **1OM** in acetonitrile, the contribution of the red-shifted TICT fluorescence is comparable to that of ^{1}t*(PICT) fluorescence, leading to a broader fluorescence spectrum. (2) Both the TICT and the ^{1}t* fluorescence of **1OM** are enhanced upon raising the temperature,[16] whereas the opposite trend is displayed by **2OM** (Figure 5). According to the scheme in Figure 7, the former can be attributed to an activated TICT fluorescence and a smaller barrier for TICT → ^{1}t* than for ^{1}t* → ^{1}p* (i.e., $E_{a1} < E_{a2}$) and the latter to weak TICT fluorescence and a larger barrier for TICT → ^{1}t* relative to that for ^{1}t* → ^{1}p* (i.e., $E_{a1} > E_{a2}$).

In addition to **2OM**, **2Me** and **2MP** also conform to $\Phi_f + 2\Phi_{tc} \ll 1$ in acetonitrile (Table 3). While this again might indicate the formation of a TICT state, the driving force is apparently much smaller than that for **2OM** based on their relative values of $\Phi_f + 2\Phi_{tc}$ (0.17−0.40 vs ~0.01). This can be readily understood based on the relative electron-donating strength of their amino groups. Since the TICT state formation is negligible for **1Me** and **1MP** in acetonitrile, the formation of a TICT state for **2Me** and **2MP** is apparently facilitated by the additional CN group. In this context, the ring-bridged compound **2MPB** serves as a rotation-inhibited model for **2MP**. The difference in fluorescence and isomerization behavior between **2MP** and **2MPB** in acetonitrile again suggests that the twisting of the stilbenyl-anilino C−N bond is responsible for the TICT state formation for **2MP** (Group II). Although the corresponding ring-bridged analogue of **2Me** was not investigated, it is reasonable to attribute its TICT state to the twisting of the same C−N bond.

The arguments applied in comparing **2OM** versus **1OM** when applied to **3MP** and **2MP** suggest that the tendency for TICT state formation should be larger in **3MP** than in **2MP** due to the stronger electron-withdrawing nitro versus cyano group. Indeed, the value of $\Phi_f + 2\Phi_{tc}$ is only 0.32 for **3MP** in THF and is expected to be much smaller in acetonitrile (Table 3). However, as indicated by **3MPB**, restriction of the rotation of the stilbenyl-anilino C−N bond does not prevent attainment of a value of $\Phi_f + 2\Phi_{tc}$ much lower than 1.0. This clearly indicates that the TICT structure for **3MP** is different from that for **2MP**. Although the exact bond that twists in **3MP** remains to be established,[32] the styryl-anilino C−C bond appears to be responsible (Group IV) based on the corresponding studies of the *N*,*N*-(dimethylamino)-derived analogue DNS (vide infra).[9]

On the other hand, the two-state (^{1}t* and ^{1}p*) model is sufficient to account for the excited-state behavior of the remaining stilbenes **2**, which conform to $\Phi_f + 2\Phi_{tc} \sim 1.0$ in both polar and nonpolar solvents (Group I). In these cases, a larger value of Φ_f is observed in more polar solvents, which is similar to the behavior of DCS but different from that of the D-only substituted stilbenes **1** and DS. The opposite trend in solvent effects on Φ_f and Φ_{tc} for DCS versus DS was previously attributed to the difference in relative polarity of the ^{1}t* versus ^{1}p* state; whereas the ^{1}p* state for DS is of zwitterionic character and more polar than its ^{1}t* state, the ^{1}p* state is less polar than the ^{1}t* state for DCS due to its biradicaloid character.[33,34] According to semiempirical calculations, the nature of ^{1}p in S_0 and S_1 is different and depends on the relative energies of the zwitterionic and biradicaloid states.[33] In other words, the biradicaloid ^{1}p state is higher in energy than the zwitterionic ^{1}p state for DCS and corresponds to S_1, but the opposite is true for DS. As a result, polar solvents stabilize the ^{1}t* state more than the ^{1}p* state for DCS and thus increase the double-bond torsional barrier and decrease the value of Φ_{tc}.[6,7] A larger double-bond torsional barrier (i.e., E_a in eq 4) is indeed observed for **2H** in acetonitrile/THF (9:1) than in methylcyclohexane. However, a larger barrier is also observed for **1H** in polar versus nonpolar solvents, which is different from the prediction for DS.[33] The relatively larger values of Φ_{tc} for **1H** in more polar solvents is apparently due to a concomitant increase in the preexponential factor, log *A*, on going from nonpolar to polar solvents, which compensates for the increased torsional barrier. In other words, a more efficient photoisomerization for **1H** in more polar solvents is not a result of a lower torsional barrier but a result of a larger torsional frequency. The same phenomenon was also observed for the solvent-dependent photoisomerization of the terminal double bond in all-*trans*-1,6-diphenyl-1,3,5-hexatriene.[35] The preexponential factor is also larger for **2H** in acetonitrile/THF (9:1) than in methylcyclohexane (Table 4). Whether this phenomenon is common for all the aminostilbenes **1** and **2** requires more thorough investigations, which are in progress in our laboratory, and the results will be reported in due course.

The formation of a TICT state for **1CN** but not for **2CN** deserves our attention. Since the aminostilbene moiety functions as the electron donor in the TICT state of **1CN** (Figure 2), the introduction of an electron-withdrawing cyano group in the donor apparently reduces its electron-donating power and thus inhibits the formation of such a DMABN-like TICT state for **2CN**. In other words, the A−D−A constitution in **2CN** disfavors the twisting of either one of the two D−A bonds.

It should also be noted that the value of μ_e determined by solvatofluorochromism for the PICT state of **2PP** (16.6 D) is as large as that for the DMABN-like TICT state of **1CN** (16.4 D).[16] Thus, a large solvatofluorochromism for D−A substituted *trans*-stilbenes does not necessarily correspond to the formation of a TICT state. In addition, both the singlet and the triplet mechanism are important in accounting for the photoisomerization of **2PP** due to its diphenylamino group.[31] This demonstrates that the parameter of $\Phi_f + 2\Phi_{tc}$ as a TICT probe for aminostilbenes is independent of the mechanism of photoisomerization. This conclusion is important for the discussion of the TICT behavior of **3MP**, **3MPB**, and DNS because the triplet-state mechanism often dominates the photoisomerization of nitro-substituted *trans*-stilbenes.[14]

Since the value of $\Phi_f + 2\Phi_{tc}$ is distinct for a TICT versus PICT state for both D-only and D−A substituted *trans*-stilbenes such as compounds **1**−**3**, it is reasonable to expect a similar behavior for the ICT states of the *N*,*N*-dimethylamino analogues DCS and DNS. Indeed, the literature values[6] of $\Phi_f + 2\Phi_{tc}$ for DCS in both nonpolar and polar solvents are close to 1.0 with the absolute values of Φ_f resembling those for **2Xy**, a compound possessing the weakest *N*-aryl amino conjugation effect among the nine derivatives of **2**. In contrast, the literature values of $\Phi_f + 2\Phi_{tc}$ are only 0.01 for DNS and *trans*-4-amino-4′-nitrostilbene (ANS) in acetonitrile.[9] Thus, the fluorescent ICT state for DCS is more likely to be planar in both nonpolar and polar solvents, but the TICT state formation appears to dominate the singlet excited decay for DNS and ANS in polar solvents. Restriction of rotation of the stilbenyl-amino C−N bond for DNS (i.e., DNSB-1) has been reported to have small effects on the values of Φ_f and Φ_{tc}, as is the case of **3MP**. Likewise, no distinct behavior was found for the double-bond constrained analogue DNSB-2. Accordingly, the TICT state of these amino-nitro disubstituted stilbenes could only result from the twisting of either the styryl-anilino C−C or the nitro-phenyl N−C single bond. However, according to the *N*-aryl amino-conjugation effect, the latter is expected to cause a smaller perturbation on Φ_f than the former. Therefore, the styryl-anilino C−C bond is more likely to be responsible for TICT state formation for amino-nitro disubstituted *trans*-stilbenes, although more concrete evidence is required to draw firmer conclusions.

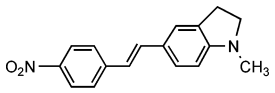

DNSB-1

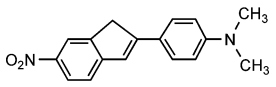

DNSB-2

Conclusion

The properties of the fluorescent ICT state of a series of arylamino-cyano disubstituted *trans*-stilbenes (**2**) and one arylamino-nitro analogue (**3MP**) have been investigated and compared with those of **1**, DCS, and DNS. As in the cases of *trans*-stilbene and many other substituted stilbenes, most of these D−A substituted stilbenes decay mainly via fluorescence and photoisomerization (i.e., $\Phi_f + 2\Phi_{tc} \sim 1$). Exceptions are found for **2OM** and **3MP** in THF and more polar solvents and for **2Me** and **2MP** in acetonitrile, where more than 50% of their excited singlet decay is via the torsion of a specific single bond to form a weakly fluorescent and isomerization-free TICT state. The TICT state for **2OM**, **2Me**, and **2MP** results from the twisting of the stilbenyl-anilino C−N bond, whereas it is more likely to be the styryl-anilino C−C single bond in the case of **3MP**. The distinct fluorescence properties of the TICT versus PICT state for *N*-aryl substituted *trans*-4-aminostilbenes conforms to the prominent amino-conjugation effect.[16,17] The characteristics of low photoisomerization quantum yield for the TICT state indicate that torsion of the single bond does not couple with that of the central double bond in the excited-state manifold. On the basis of the behavior of **1**−**3**, a rule of thumb for judging the importance of a TICT state for *trans*-stilbenes was deduced: the presence of a low-lying TICT state in polar but not in nonpolar solvents corresponds to $\Phi_f + 2\Phi_{tc} \sim 1$ in nonpolar solvents such as hexane, $\Phi_f + 2\Phi_{tc} \ll 1$ in polar solvents such as acetonitrile, and to a large ratio of Φ_f in nonpolar versus polar solvents (e.g., $\Phi_f(\text{Hex})/\Phi_f(\text{MeCN}) > 50$). Accordingly, the TICT state formation is important for DNS ($\Phi_f + 2\Phi_{tc} \sim 0.89$ in cyclohexane and ~0.1 in acetonitrile and $\Phi_f(\text{Hex})/\Phi_f(\text{MeCN}) > 165$) but not for DCS ($\Phi_f + 2\Phi_{tc} \sim 0.93$ in both cyclohexane and acetonitrile and $\Phi_f(\text{Hex})/\Phi_f(\text{MeCN}) < 1$). For cases that possess intermediate values of $\Phi_f + 2\Phi_{tc}$ and $\Phi_f(\text{Hex})/\Phi_f(\text{MeCN})$ such as **2MP** ($\Phi_f +$

$2\Phi_{tc} \sim 0.5$ in acetonitrile and $\Phi_f(\text{Hex})/\Phi_f(\text{MeCN}) \sim 1$), TICT state formation is nonnegligible but rather inefficient. It should be noted that although our results indirectly support the previously proposed TICT structure for DNS, where the styryl-anilino C−C single bond is twisted,[8,10] the nonemissive nature of the TICT state revealed herein conforms to the classical TICT model[2,19] rather than to the highly emissive one that was proposed.[8,10] In addition, our preliminary studies on the activation parameters for **1H** and **2H** indicate that both D-only and D−A substituted *trans*-stilbenes have larger barriers for olefinic bond torsion in more polar solvents. Thus, the difference in solvent effects on Φ_f and Φ_{tc} is mainly due to the difference in the preexponentials rather than to the difference in the relative polarity of ^{1}t* versus ^{1}p*. Continued efforts toward a better understanding of this issue for the other D-only and D−A substituted *trans*-stilbenes are in progress.

Acknowledgment. Financial support for this research was provided by the National Science Council of Taiwan, ROC.

Supporting Information Available: Synthetic schemes, characterization data for new compounds, solvatofluorochromic plots for **2** and **3**, and temperature-dependent absorption spectra for **2H** and **2OM**. This material is available free of charge via the Internet at http://pubs.acs.org.

References and Notes

(1) (a) Lippert, E.; Lüder, W.; Moll, F.; Nägle, W.; Boos, H.; Prigge, H.; Seibold-Blankenstein, I. *Angew. Chem.* **1961**, *73*, 695−706. (b) Lippert, E.; Lüder, W.; Boos, H. In *Advances in Molecular* Spectroscopy; Mangini, A., Ed.; Pergamon Press: Oxford, 1962; pp 443−457.

(2) (a) Rotkiewicz, K.; Grellmann, K. H.; Grabowski, Z. R. *Chem. Phys. Lett.* **1973**, *19*, 315−318. (b) Rettig, W. *Angew. Chem., Int. Ed. Engl.* **1986**, *25*, 971−988. (c) Rettig, W.; Maus, M. In *Conformational Analysis of Molecules in Excited States*; Waluk, J., Ed.; Wiley-VCH: New York, 2000; Ch. 1, pp 1−55. (d) Grabowski, Z. R.; Rotkiewicz, K. *Chem. Rev.* **2003**, *103*, 3899−4031.

(3) (a) Jödicke, C. J.; Lüthi, H. P. *J. Am. Chem. Soc.* **2003**, *125*, 252−264. (b) Rappoport, D.; Furche, F. *J. Am. Chem. Soc.* **2004**, *126*, 1277−1284. (c) Gómez, I.; Reguero, M.; Boggio-Pasqua, M.; Robb, M. A. *J. Am. Chem. Soc.* **2005**, *127*, 7119−7129. (d) Minezawa, N.; Kato, S. *J. Phys. Chem. A* **2005**, *109*, 5445−5453. (e) Amatatsu, Y. *J. Phys. Chem. A* **2005**, *109*, 7225−7235.

(4) (a) von der Haar, T.; Hebecker A.; Il'ichev, Y. V.; Jiang, Y.-B.; Kühnle, W.; Zachariasse, K. A. *Recl. Trav. Chim. Pays-Bas* **1995**, *114*, 430−442. (b) Zachariasse, K. A.; Grobys, M.; von der Haar, T.; Hebecker, A.; Il'ichev, Y. V.; Jiang, Y.-B.; Morawski, O.; Kühnle, W. *J. Photochem. Photobiol., A* **1996**, *102*, 59−70. (c) Zachariasse, K. A.; Grobys, M.; von der Haar, T.; Hebecker A.; Il'ichev, Y. V.; Morawski, O.; Rückert, I.; Kühnle, W. *J. Photochem. Photobiol., A* **1997**, *105*, 373−383. (d) Il'ichev, Y. V.; Kühnle, W.; Zachariasse, K. A. *J. Phys. Chem.* **1998**, *102*, 5670−5680. (e) Zachariasse, K. A. *Chem. Phys. Lett.* **2000**, *320*, 8−13. (f) Demeter, A.; Zachariasse, K. A. *Chem. Phys. Lett.* **2003**, *380*, 699−703. (g) Zachariasse, K. A.; Druzhinin, S. I.; Bosch, W.; Machinek, R. *J. Am. Chem. Soc.* **2004**, *126*, 1705−1715. (h) Techert, S.; Zachariasse, K. A. *J. Am. Chem. Soc.* **2004**, *126*, 5593−5600.

(5) (a) Safarzadeh-Amiri, A. *Chem. Phys. Lett.* **1986**, *125*, 272−278. (b) Rechthaler, K.; Köhler, G. *Chem.* Phys. *Lett.* **1996**, *250*, 152−158. (c) Eilers-König, N.; Kühne, T.; Schwarzer, D.; Vöhringer, P.; Schroeder, J. *Chem. Phys. Lett.* **1996**, *253*, 69−76. (d) Kovalenko, S. A.; Schanz, R.; Senyushkina, T. A.; Ernsting, N. P. *Phys. Chem. Chem. Phys.* **2002**, *4*, 703−707.

(6) Gruen, H.; Görner, H. *Z. Naturforsch.* **1983**, *38*, 928−936.

(7) (a) Il'ichev, Y. V.; Kühnle, W.; Zachariasse, K. A. *Chem. Phys.* **1996**, *211*, 441−453. (b) Il'ichev, Y. V.; Zachariasse, K. A. *Ber. Bunsen-Ges. Phys. Chem.* **1997**, *101*, 625−635. (c) Lewis, F. D.; Weigel, W. *J. Phys. Chem. A* **2000**, *104*, 8146−8153.

(8) (a) Gilabert, E.; Lapouyade, R.; Rullière, C. *Chem. Phys. Lett.* **1988**, *145*, 262−268. (b) Rettig, W.; Majenz, W. *Chem. Phys. Lett.* **1989**, *154*, 335−341. (c) Lapouyade, R.; Czeschka, K.; Majenz, W.; Rettig, W.; Gilabert, E.; Rullière, C. *J. Phys. Chem.* **1992**, *96*, 9643−9650. (d) Abraham, E.; Oberlé, J.; Jonusauskas, G.; Lapouyade, R.; Rullière, C. *J. Photochem. Photobiol., A* **1997**, *105*, 101−107. (e) Abraham, E.; Oberlé, J.; Jonusauskas, G.; Lapouyade, R.; Rullière, C. *Chem. Phys.* **1997**, *214*, 409−423. (f) Amatatsu, Y. *Theor. Chem. Acc.* **2000**, *103*, 445−450. (g) Amatatsu, Y. *Chem. Phys.* **2001**, *274*, 87−98. (h) Pines, D.; Pines, E.; Rettig, W. *J. Phys. Chem. A* **2003**, *107*, 236−242.

(9) Gruen, H.; Görner, H. *J. Phys. Chem.* **1989**, *93*, 7144−7152.

(10) (a) Lapouyade, R.; Kuhn, A.; Létard, J.-F.; Rettig, W. *Chem. Phys. Lett.* **1993**, *208*, 48−58. (b) Peinado, C.; Salvador, E. F.; Catalina, F.; Lozano, A. E. *Polymer* **2001**, *42*, 2815−2825.

(11) (a) Saltiel, J.; Charlton, J. L. In *Rearrangements in Ground and Excited States*; de Mayo, P., Ed.; Academic Press: New York, 1980; Vol. 3, pp 25−89. (b) Saltiel, J.; Sun, Y.-P. In *Photochromism, Molecules and Systems*; Dürr, H., Bouas-Laurent, H., Eds.; Elsevier: Amsterdam, 1990; pp 64−164.

(12) Waldeck, D. H. *Chem. Rev.* **1991**, *91*, 415−436.

(13) Meier, H. *Angew. Chem., Int. Ed. Engl.* **1992**, *31*, 1399−1420.

(14) Görner, H.; Kuhn, H. J. *Adv. Photochem.* **1995**, *19*, 1−117.

(15) Papper, V.; Likhtenshtein, G. I. *J. Photochem. Photobiol., A* **2001**, *140*, 39−52.

(16) Yang, J.-S.; Liau, K.-L.; Wang, C.-M.; Hwang, C.-Y. *J. Am. Chem. Soc.* **2004**, *126*, 12325−12335.

(17) (a) Yang, J.-S.; Chiou, S.-Y.; Liau, K.-L. *J. Am. Chem. Soc.* **2002**, *124*, 2518−2527. (b) Yang, J.-S.; Wang, C.-M.; Hwang, C.-Y.; Liau, K.-L.; Chiou, S.-Y. *Photochem. Photobiol. Sci.* **2003**, *2*, 1225−1231.

(18) Létard, J.-F.; Lapouyade, R.; Rettig, W. *J. Am. Chem. Soc.* **1993**, *115*, 2441−2447.

(19) (a) Seydack, M.; Bendig, J. *J. Phys. Chem. A* **2001**, *105*, 5731−5733. (b) Maliakal, A.; Lem, G.; Turro, N. J.; Ravichandran, R.; Suhadolnik, J. C.; DeBellis, A. D.; Wood, M. G.; Lau, J. *J. Phys. Chem. A* **2002**, *106*, 7680−7689. (c) Nad, S.; Kumbhakar, M.; Pal, H. *J. Phys. Chem. A* **2003**, *107*, 4808−4816. (d) Paterson, M. J.; Robb, M. A.; Blancafort, L.; DeBellis, A. D. *J. Am. Chem. Soc.* **2004**, *126*, 2912−2922.

(20) (a) Wolfe, J. P.; Wagaw, S.; Marcoux, J.-F.; Buchwald, S. L. *Acc. Chem. Res.* **1998**, *31*, 805−818. (b) Hartwig, J. F. *Angew. Chem., Int. Ed. Engl.* **1998**, *37*, 2046−2067.

(21) Dawson, W. R.; Windsor, M. W. *J. Phys. Chem.* **1968**, *72*, 3251−3260.

(22) Zerner, M. C.; Leow, G. H.; Kirchner, R. F.; Mueller-Westerhoff, U. T. *J. Am. Chem. Soc.* **1980**, *102*, 589−599.

(23) Baumann, W.; Bischof, H.; Fröhling, J.-C.; Brittinger, C.; Rettig, W.; Rotkiewicz, K. *J. Photochem. Photobiol., A* **1992**, *64*, 49−72.

(24) Dewar, M. J. S.; Zoebisch, E. G.; Healy, E. F.; Stewart, J. J. P. *J. Am. Chem. Soc.* **1985**, *107*, 3902−3909.

(25) Lowry, T. H.; Richardson, K. S. *Mechanism and Theory in Organic Chemistry*; Harper and Row: New York, 1987; p 144.

(26) The fluorescence spectra are uncorrected for the temperature dependence of the absorbance. Nonetheless, the reduction of fluorescence is larger than 75% for all cases on going from −40 to 40 °C, but the corresponding change in absorbance at the excitation wavelength is less than 15% for all cases (see Supporting Information for the spectra).

(27) Although the value of Φ_{tc} for **3MP** and **6H** in solvents more polar than THF was not determined, it is expected to be low and the sum of $\Phi_f + 2\Phi_{tc}$ much lower than 1.0 in view of the low values of Φ_f.

(28) Lewis, F. D.; Zuo, X. *J. Am. Chem. Soc.* **2003**, *125*, 2046−2047.

(29) Lewis, F. D.; Zuo, X. *J. Am. Chem. Soc.* **2003**, *125*, 8806−8813.

(30) The values of Σk and k_d in methylcyclohexane and MeCN/THF (9:1) are compared with the values of k_f and k_{nr} in hexane and MeCN, respectively.

(31) Yang, J.-S.; Liau, K.-L.; Tu, C.-W.; Hwang, C.-Y. *J. Phys. Chem. A* **2005**, *109*, 6450−6456.

(32) An attempt to prepare the C−C bond constrained ring-bridged analogue for **3MP** was unfortunately unsuccessful.

(33) Rettig, W.; Strehmel, B.; Majenz, W. *Chem. Phys.* **1993**, *173*, 525−537.

(34) Papper, V.; Pines, D.; Likhtenshtein, G.; Pines, E. *J. Photochem. Photobiol., A* **1997**, *111*, 87−96.

(35) Saltiel, J.; Krishnamoorthy, G.; Huang, Z.; Ko, D.-H.; Wang, S. *J. Phys. Chem. A* **2003**, *107*, 3178−3186.